J Mater Sci (2009) 44:3408–3412
DOI 10.1007/s10853-009-3452-5

# Microstructure and mechanical properties of nanolayered W/W–C thin films

**K. Abdelouahdi · C. Legrand-Buscema · P. Aubert**

Received: 20 January 2009 / Accepted: 31 March 2009 / Published online: 17 April 2009


**Abstract** The present study reports on the mechanical and structural properties of W/W–C multilayered thin films with bilayer periods Λ ranging from 2.5 to 100 nm. Films were grown by reactive sputtering radio frequency on Si (100) substrate. X-ray diffraction (XRD), grazing incidence X-ray diffraction (GIXRD) and X-ray reflectivity were used to globally characterise the multilayers structure. Hardness and Young modulus have been determined using nanoindentation with a Berkovich tip. The XRD and the GIXRD diagrams revealed the presence of three phases: $WC_{1-x}$ randomly oriented, $W_2C$ with (100) preferred orientation and W with (110) preferred orientation. An increase in hardness is observed with decreasing period Λ, reaching a maximum value of $\sim$26 GPa at $\Lambda = 2.5$ nm.

## Introduction

Multilayer films with nanometric periods are known to improve the mechanical properties of thin film coatings by increasing their hardness or toughness and by relaxing the film stresses. They can also improve the tribological properties by increasing the coating/substrate adhesion, the load support and the resistance to crack propagation [1, 2]. Various models have been proposed to explain the hardness enhancement such as dislocation pile-ups at interfaces or grain boundaries [3]. Recently, Verdier [4] has reported a modelling using dislocation dynamic simulation adapted to the composite structure.

K. Abdelouahdi (✉) · C. Legrand-Buscema · P. Aubert
Laboratoire d'étude des Milieux Nanométriques, Université d'Evry Val d'Essonne, 91025 Evry Cedex, France
e-mail: karima505@yahoo.fr

Transition metal carbides like tungsten carbide present a high technological interest due to many of their specific physical and mechanical properties [5]. Tungsten, in the metal form, is another material frequently used due to its high melting point temperature and high hardness [6]. The combination of tungsten carbide and tungsten coatings to form a nanolayers thin films system was then proposed in this study.

In a previous work [7], we reported the deposition of monolithic W–C obtained by radio frequency (RF) reactive sputtering. The coating presenting $WC_{1-x}$ phase randomly oriented exhibited a good structural and mechanical properties. Thus, the deposition conditions of this coating were retained for the multilayers elaboration.

In the present work, we investigate the structure of this multilayers and the impact of the periodicity (Λ = thickness of neighbouring bi-layers of W–C and W) on the mechanical properties of the W/W–C multilayers.

## Experimental details

### Coatings deposition

The multilayers are deposited on (100) oriented silicon wafers by RF sputtering from a pure tungsten target W (5 N). The samples are placed 7 cm away from the target and heated to 150 °C (this temperature is required to obtain a crystalline film). The overall sputtering pressure is fixed at 0.25 Pa for all the experiments, and the sputtering RF power is 200 W, leading to a –400 V self-bias. According to the deposited layer, i.e. either W or W–C, the sputtering gas was pure Ar or a $CH_4$ + Ar mixture, respectively. For elaboration of WC layer, the percentage of $CH_4$ was close to 2% of the total pressure. The elaboration of W/W–C

multilayers is operated in the same deposition step, the change of single-layer material, i.e. from W to W–C or from W–C to W, is obtained by switching on or off the methane gas in the sputtering chamber.

A series of W/W–C multilayers are produced with periods (Λ) ranging from 2.5 to 100 nm, the total film thickness is approximately 300 nm for mechanical studies and less than 100 nm for X-ray reflectometry (XRR) studies.

### Microstructural and mechanical characterizations

The crystallographic structure of samples was studied by X-ray diffraction (XRD) (D8, Brucker). The both conventional Bragg–Brentano and grazing incidence X-ray diffraction (GIXRD) arrangements can be exploited. The patterns are performed in the same conditions (step size = 0.04°, time by step = 30 s).

The combination of GIXRD with $\theta - 2\theta$ XRD is used for evaluating crystallinity and characterizing the different phases of WC (i.e. $W_2C$, $WC_{1-x}$ and WC), which allows to put in evidence the preferential orientations of the coatings.

The real period thickness, the interface roughness and density of the multilayers are obtained by the simulation of XRR diagrams with Refsim program.

Mechanical properties of the multilayers are determined through hardness measurements, which are carried out using a Hysitron triboscope nanomechanical system with a maximal force equal to 10 mN. This device is connected to a digital instruments D 3100 AFM. A pyramidal diamond Berkovich tip is used for visualization and tests. Hardness $H$ is deduced from the Oliver and Pharr analysis method [8]. In order to avoid the influence of the substrate, the penetration depth is always kept below 10% of the layer thickness. The applied force used for this is 1 mN. All the data given in this study correspond to an average of 20 measurements.

## Results and discussion

### Structural study

Figure 1 presents the XRR diagrams of W/W–C multilayers with Λ = 2.5, 5, 8, 10, 15 and 20 nm.

For all the samples, Bragg's peaks of multiple orders are presented and confirm the composition modulation. Nevertheless, the intensity of these peaks is more pronounced in the case of the thin periods (i.e. Λ = 2.5, 5, 8 and 10 nm). Indeed, the number of interfaces in this case is important (40, 20, 12 and 10, respectively), thus, Bragg's peaks of multiple order are more intense. Whereas in the case of the thick periods (i.e. Λ = 15 and 20 nm), the small number of interfaces (6 and 5) is responsible of the low

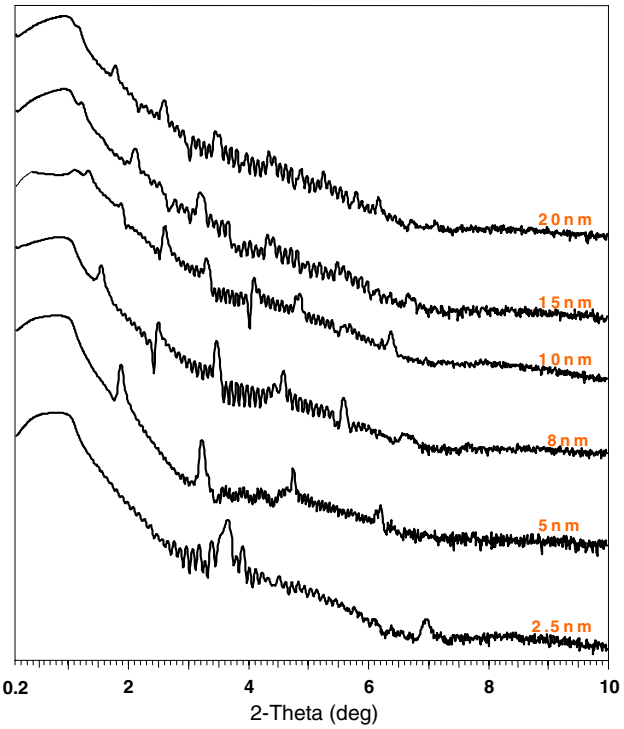


**Fig. 1** XRR patterns of $[W/W–C]_n$ multilayers for different periods Λ = 2.5, 5, 8, 10, 15 and 20 nm

Bragg's peaks intensity. Furthermore, the densities of the monolayers WC ($WC_{1-x}$ (17.2), $W_2C$ (17.1)) and W (19.2) are very close to precisely determine the number of period ($N$) and to perform a good fits of the XRR diagrams. The XRD patterns of W/W–C multilayers thin films are displayed in Fig 2. On all diagrams, the high relative intensity of (110) W peak masks the other peaks. For this reason, we have presented (on the right of Fig. 2) the enlargement of the XRD pattern of the multilayer with Λ = 100 nm. This diagram shows four peaks, which can be attributed to (100) $W_2C$, (111) $WC_{1-x}$, (110) W and (200) $WC_{1-x}$, respectively, with Bragg angle values equal to $2\theta = 34.16°$, $2\theta = 36.27°$, $2\theta = 39.91°$ and $2\theta = 42.02°$. The GIXRD patterns corresponding are presented in Fig. 3. Two grazing angles are chosen 0.5° and 1.5°. These angles allow to analyze a depth of about 50 and 150 nm, respectively, in W–C layer (depths calculated for $WC_{1-x}$ phase). Consequently, for a period Λ of 100 nm, an angle of 0.5° (Fig. 3a) reveals only tungsten carbide layer, while an angle of 1.5° (Fig. 3b) allows to characterize both layers (W/WC) corresponding to the period.

For comparison, the GIXRD diagram of monolithic W–C film is presented too (Fig. 3c).

Like what we have presented in a previous work [7], we considered that the relative intensities of the $WC_{1-x}$ are different of these indicated in the powder diffraction file 20-1316. Indeed, we have demonstrated that in the

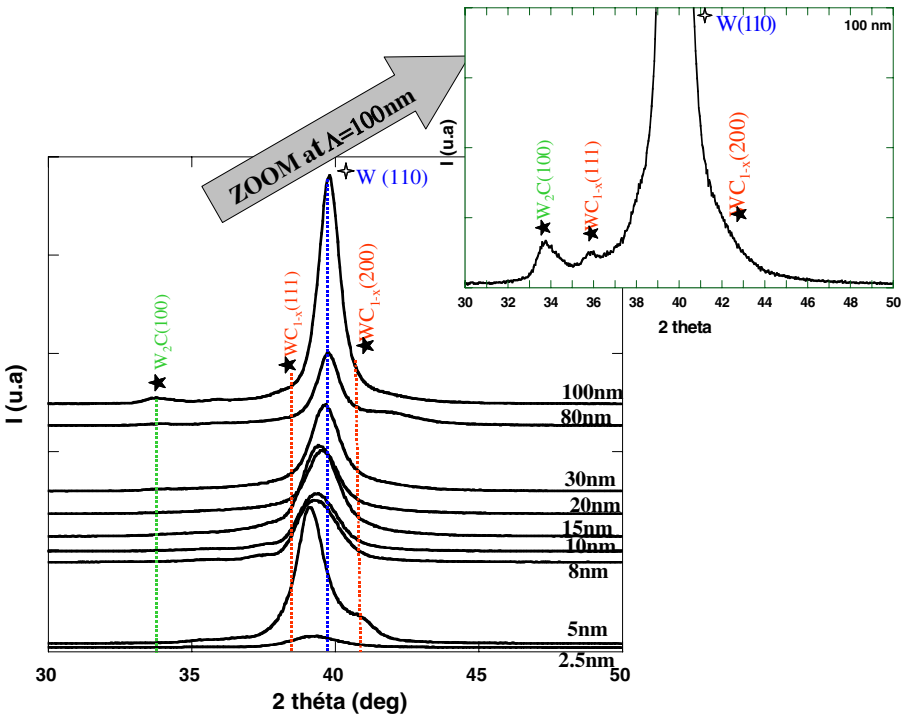


**Fig. 2** XRD diagrams of $[W/W–C]_n$ multilayers for different periods $\Lambda = 2.5$, 5, 8, 10, 15, 20, 30, 80 and 100 nm

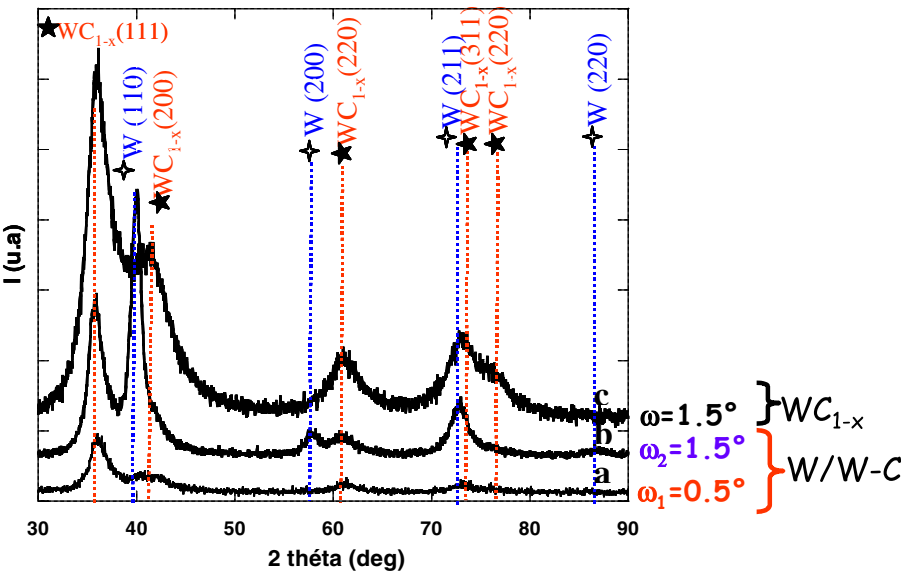


**Fig. 3** GIXRD patterns of W/W–C multilayers for a period $\Lambda = 100$ nm (**a** and **b**) and W–C monolayer ($WC_{1-x}$ phase) (**c**)

structure of $WC_{1-x}$ (Fm3m like NaCl) the highest intensity is for (111) reflection. So, Fig. 3c indicates that the $WC_{1-x}$ phase is randomly oriented.

Clear diffraction peaks of W Wolfram [(110) (200) and (210)] are observed in Fig. 3b, while in Fig. 3a only the diffraction peaks of $WC_{1-x}$ [(111) (200) (220) and (311)] are present like Fig. 3c corresponding to the W–C monolayer. GIXRD method characterizes the disoriented phase crystallized or crystalline phases presenting a preferential orientation with wide rocking-curve's FWHM of some degrees. The comparison between XRD and GIXRD patterns shows that tungsten layers are crystallized in a cubic structure with a {110} preferential orientation, whereas two phases of tungsten carbide exist: the cubic phase $WC_{1-x}$ randomly oriented and the hexagonal phase $W_2C$ with {100} texture.

As a matter of fact, an epitaxial relationship can exist between $W_2C$ and W. Indeed, the (100) of the hexagonal structure $W_2C$ ($a = 0.2997$ nm, $c = 0.4727$ nm) presents a lattice mismatch of 5.3% along [010] direction and 5.6%

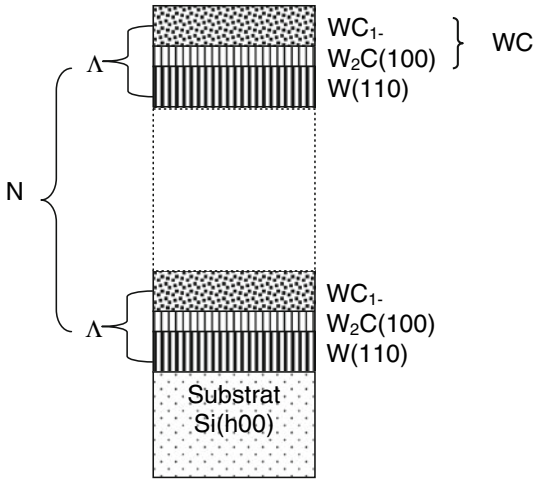


**Fig. 4** Structure of $[W/W–C]_n$ multilayers thin films

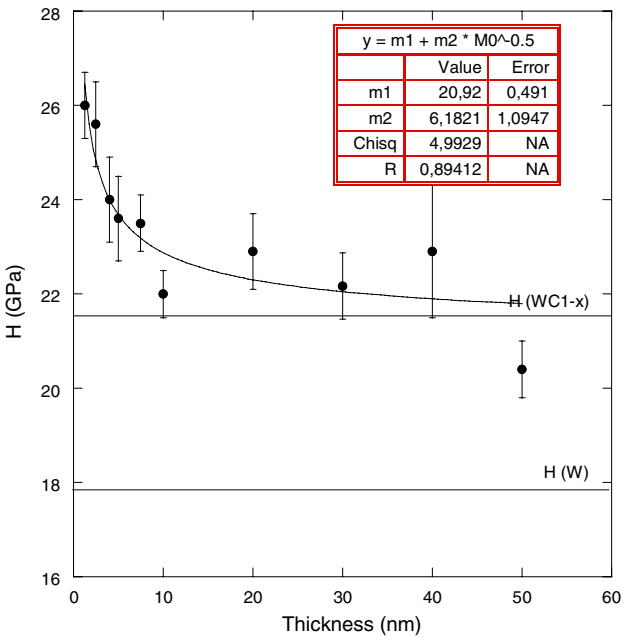


**Fig. 5** Hardness versus tungsten thickness in multilayers

along [001] direction with the (110) of the cubic structure W ($a = 0.31648$ nm). The absence of the peak (100) $W_2C$ in GIXRD results shows the strong preferential orientation but, in this case, the rocking curve of (100) $W_2C$ ($2\theta = 34.52°$) is not realizable because of the two peaks of diffraction: (111) $WC_{1-x}$ and (110) W, appearing in the same range of 32°–39° ($2\theta$).

This explains the presence of the phase $W_2C$ in $[W–C/W]_n$ multilayers while in monolayer only the $WC_{1-x}$ phase was formed [7]. The $W_2C$ phase oriented according to the preferential orientation (100) is localized at the interface as in Fig. 4.

We make the assumption that the $W_2C$ layer is very thin to keep oriented in W while the W layer presents a strong disorientation.

So afterwards, for the characterization of the mechanical properties of these multilayers, we do not take into account the presence of $W_2C$ phase.

## Mechanical properties

The hardness given is reported in Fig. 5. The hardness increases with decreasing period thickness to go beyond the rule-of-mixture (19.5 GPa) value for samples with period thickness $\Lambda \leq 100$ nm. The maximum hardness value (26 GPa), in the range investigated here, is obtained for the smallest period thickness (i.e. 2.5 nm). Similar behaviours have been reported for TiN/Ti, WN/W [9, 10]. This is in agreement with those studies [9, 10] where the critical period thickness is found in the range of 2–3 nm. Thus, deposition of samples with $\Lambda$ less than 2.5 nm should give more information about this aspect.

The hardness behaviour of multilayers with period in the nanometre scale has been the subject of many investigations. In particular, in the range $\Lambda \leq 100$ nm, there are some behaviours commonly observed for all the systems studied. First, the hardness increases as the period decreases until a critical value. The maximum hardness obtained is, in all cases, greater than rule-of-mixture value. Second, below this critical period, the hardness remains constant or, in most cases, decreases as the period decreases. The decrease of hardness is attributed to the lack of multilayering character and the decrease of the composition modulation amplitude due to the mixing and the inter-diffusion.

The explanation of hardness enhancement is based on plastic deformation and more precisely on dislocation motion: Hall–Petch and Orowan mechanisms of strengthening [11].

According to Misra et al. [12, 13], we can obtain limiting values of microstructural scales at which these different mechanisms operate. This approach is based on estimation of back stress due to misfit dislocations at interfaces and pile up at boundaries grains.

This model presents an approach of deformation mechanisms and only serves as guidelines. To construct this model, we must use misfit strain, burger vector, shear modulus and poisson's ratio of the softer layer, which is measured in monolayer samples or extracts to bulk data. This sample map is in good agreement with experimental data but more information as structural properties, difference of shear moduli will be done if we want to use this model to a universal model.

We present these results in the form of two-dimensional map of layers thickness $h$ and grain size $d$ ranges using the experimental values of Young modulus of monolithic W

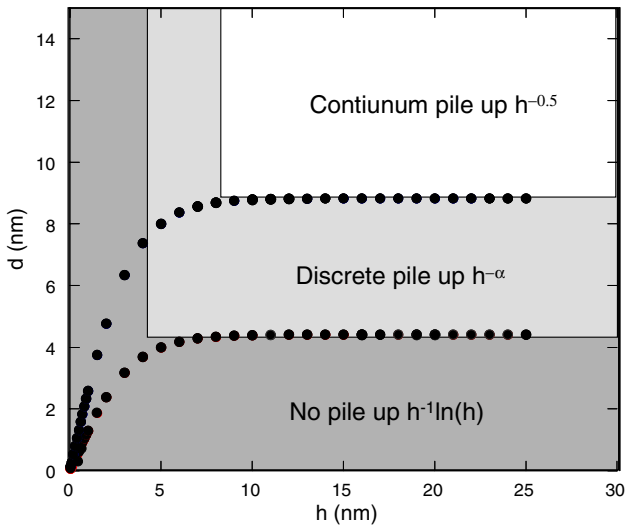


**Fig. 6** Deformation mechanism map for W/W–C multilayers ($d$ and $h$ are, respectively, tungsten grain size and its thickness)

and $WC_{1-x}$. In our case, ignoring any possible strain broadening contribution, an average grains size can be estimated from the Scherrer formula from Figs. 2, 3. The estimated W and $WC_{1-x}$ grain size is close to 10 nm. The different deformation mechanism is shown in the map (Fig. 6). The deformation occurs in the plastically softer phase W, and hardening is due to the elastically stiffer phase $WC_{1-x}$. In this case, interfaces are considered impenetrable, chemically sharp, which is not necessarily the case of partially miscible layers like W and $WC_{1-x}$. So, the effect of gradual interface and composition profile on the hardness behaviour is not considered.

Taking into account the grains size and the multilayers period, the deformation mechanism is due to pile up dislocations effects at the interfaces. In our case, hardness enhancement is due to a continuum pile up with a tungsten-thickness dependence. The data give a better fit with relationship similar to $H = H_0 + k \times \Lambda^{-0.5}$.

For a large multilayer period, hardness ($m_1$) is close to tungsten hardness $H_0$. We can compare hardening fit constant ($m_2$) to Hall–Petch computing constant using equation $k = 0.2G\sqrt{b}$ where $b$ is the Burgers vector and $G$ the shear modulus of elastically stiffer phase. The result give $k = 7.5$ comparing to $m_2 = 6.2$.

## Conclusion

W/W–C multilayers with periods $\Lambda$ ranging from 2.5 to 100 nm have been synthesized using reactive sputtering RF The structure of the multilayers consists on the W preferentially oriented (110) in the tungsten layer, a thin layer constituted of $W_2C$ preferentially oriented (100) at the interface and the $WC_{1-x}$ randomly oriented in W–C layer. The appearance of the $W_2C$ phase is due to the low lattice mismatch between the (100) planes of $W_2C$ and the (110) planes of W. Hardness values are found to be larger than the rule of mixture value (19.5 GPa); however, an increase is observed with decreasing $\Lambda$, the maximum hardness being 26 GPa obtained at $\Lambda = 2.5$ nm. This behaviour can be explained by the Hall–Petch mechanism.

## References

1. Kong M, Shao N, Dong Y, Yue J, Li G (2006) Mater Lett 60:874
2. Bejarano G, Caicedo JM, Baca E, Prieto P, Balogh AG, Enders S (2006) Thin Solid Films 494:53
3. Koehler JS (1978) Phys Rev B 2:547
4. Verdier M (2004) Scr Mater 50:769
5. Toth LE (1971) Handbook of transition metal carbides and nitrides. Academic Press, New York and London
6. Smallwood RE (1982) Refractory metals and their industrial applications. ASTM Committee B-10 on Reactive and Refractory Metals and Alloys, Philadelphia, PA, p 82
7. Abdelouahdi K, Sant C, Miserque F, Aubert P, Zhen Y, Legrand-Buscema C, Perrière J (2006) J Phys Condens Matter 18:1913
8. Oliver WC, Pharr GM (1992) J Mater Res 7:1564
9. Maillé L, Aubert P, Sant C, Garnier P (2004) Surf Coat Technol 180–181:483
10. Ben Daia M, Aubert P, Labdi S, Sant C, Sadi FA, Houdy P (2000) J Appl Phys 87:7753
11. Was GS, Foecke T (1996) Thin Solid Films 286:1
12. Misra A, Verdier M, Kung H, Embury JD, Hirth JP (1999) Scr Mater 41:973
13. Misra A, Verdier M, Lu YC, Kung H, Mitchell TE, Nastasi M, Embury JD (1998) Scr Mater 39:555